John von Neumann Institute for Computing

Many-Body Perturbation Theory: The *GW* Approximation

Christoph Friedrich and Arno Schindlmayr

published in

Computational Nanoscience: Do It Yourself!,
J. Grotendorst, S. Blügel, D. Marx (Eds.),
John von Neumann Institute for Computing, Jülich,
NIC Series, Vol. **31**, ISBN 3-00-017350-1, pp. 335-355, 2006.

http://www.fz-juelich.de/nic-series/volume31

Many-Body Perturbation Theory: The *GW* Approximation

Christoph Friedrich and Arno Schindlmayr

Institute of Solid State Research
Forschungszentrum Jülich
52425 Jülich, Germany
E-mail: {*c.friedrich, a.schindlmayr*}*@fz-juelich.de*

In this lecture we present many-body perturbation theory as a method to determine quasiparticle excitations in solids, especially electronic band structures, accurately from first principles. The main ingredient is the electronic self-energy that, in principle, contains all many-body exchange and correlation effects beyond the Hartree potential. As its exact mathematical expression is unknown, approximations must be used in practical calculations. The *GW* approximation is obtained using a systematic algebraic approach on the basis of Green function techniques. It constitutes an expansion of the self-energy up to linear order in the screened Coulomb potential, which describes the interaction between the quasiparticles and includes dynamic screening through the creation of exchange-correlation holes around the bare particles. The implementation of the *GW* approximation relies on a perturbative treatment starting from density functional theory. Besides a detailed mathematical discussion we focus on the underlying physical concepts and show some illustrative applications.

1 Introduction

In the previous lectures we have seen that density functional theory (DFT) is the method of choice when we are interested in the ground-state properties of a many-electron system. DFT is based on the Hohenberg-Kohn theorem,[1] which states that there is (a) a one-to-one correspondence between the ground-state density $n_0(\mathbf{r})$ and the external potential as well as (b) a variational principle for the energy functional $E[n_0] \leq E[n]$. The second statement allows to obtain the ground state of a many-electron system by variation of its density, a quantity that is much less complicated than the many-electron wave function $\Psi_0(\mathbf{r}_1, \ldots, \mathbf{r}_N)$, where N is the particle number. The first statement implies that the many-particle Hamiltonian is a functional of the ground-state density. Since the diagonalization of the Hamiltonian yields the complete excitation spectrum, the excited states can ultimately be regarded as functionals of the ground-state density as well. However, the Hohenberg-Kohn theorem does not provide us with an explicit mathematical form. In this lecture we show that excited-state properties can be accessed more directly with a purpose-built method, the so-called many-body perturbation theory.[2,3] Incidentally, in practice its implementation within the *GW* approximation[4] for the electronic self-energy is based on a perturbative evaluation with Kohn-Sham orbitals and can, therefore, finally be interpreted as the desired density functional.

The solution of the Kohn-Sham equation[5] of DFT yields a whole spectrum of single-particle states, and one is tempted to identify the corresponding eigenvalues with excitation energies. Strictly speaking, such an interpretation is wrong: the Kohn-Sham wave functions and eigenvalues must be considered as mathematical tools and cannot be endowed with a physical meaning. The only exception is the energy of the highest occupied state,

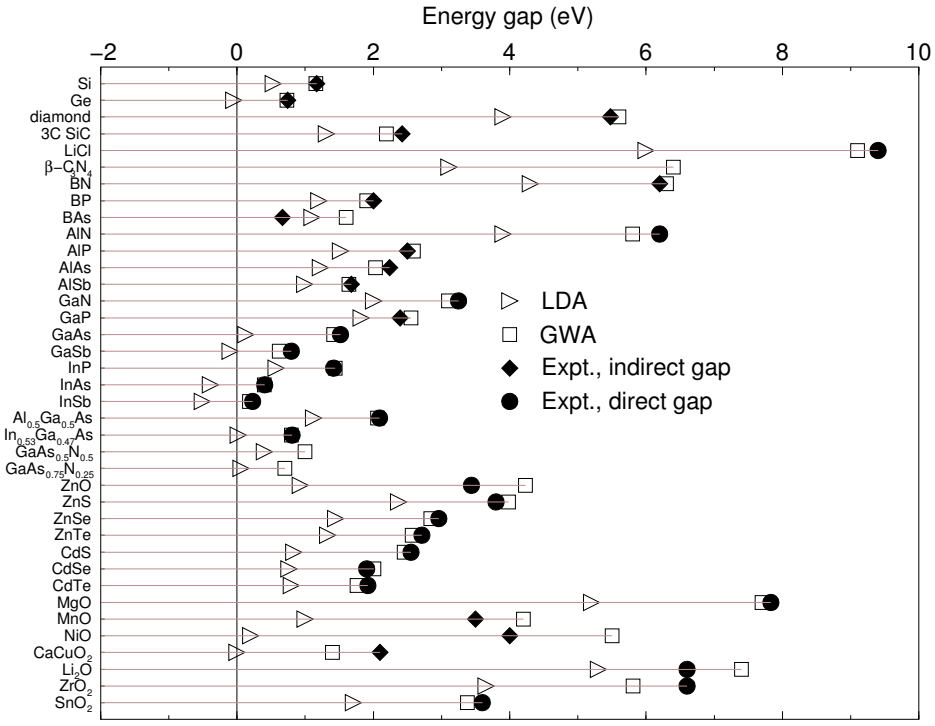

Figure 1. Comparison of LDA, GW and experimental band gaps for a variety of materials. Taken from Ref. 8.

which equals the exact ionization potential (or chemical potential for metals).[6,7] Consequently, while often qualitatively correct, the DFT band structure fails to give reliable quantitative values for the band gaps of insulators and semiconductors, which are often underestimated by as much as 1.0 eV or more. In the case of Ge the local-density approximation (LDA) of DFT even predicts a semi-metal with a negative band gap rather than a semiconductor. In this lecture we demonstrate that the Kohn-Sham eigenvalues can be corrected using Green function techniques and the GW approximation for the electronic self-energy. Figure 1 shows a comparison of LDA and self-energy corrected band gaps with respective experimental values for a variety of materials. The underestimation within the LDA as well as the improvement by the GW approximation are evident.

Band gaps are experimentally measured by photoelectron spectroscopy. Figure 2 gives a schematic illustration. In direct photoelectron spectroscopy a photon with energy $\hbar\omega$ impinges on the sample and ejects an electron, whose kinetic energy $E_{\rm kin}$ is subsequently measured. The binding energy ϵ_i of this electron is given by the difference $\epsilon_i = E_{\rm kin} - \hbar\omega$. Actually, we already simplified the argumentation here, as the formulation "binding energy of an electron" suggests that the electrons are independent. In reality they are correlated through the Coulomb interaction, and the ejection of an electron is always a many-body process. In this general sense ϵ_i equals the difference $\epsilon_i = E_0^N - E_i^{N-1}$ between the total energy E_0^N of the N-particle ground state Ψ_0^N and the energy E_i^{N-1} of the $(N-1)$-particle state Ψ_i^{N-1} that remains after the emission. Inverse photoelectron spectroscopy is

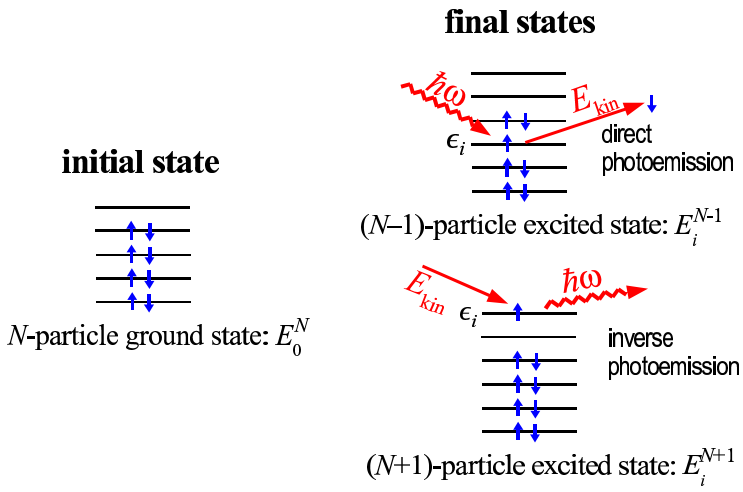

Figure 2. Schematic illustration of direct and inverse photoelectron spectroscopy. In both processes the particle number changes. The measured energy difference $E_{\rm kin} - \hbar\omega$ corresponds to $\epsilon_i = E_0^N - E_i^{N-1}$ in direct and $\epsilon_i = E_i^{N+1} - E_0^N$ in inverse photoelectron spectroscopy.

the complementary process: electrons are injected into the sample, and the energy of the emitted photon is measured. The number of electrons in the system thus increases from N to $N+1$, and we can identify $E_{\rm kin} - \hbar\omega$ with the energy difference $\epsilon_i = E_i^{N+1} - E_0^N$ of the many-electron systems.

The fact that the independent-electron picture breaks down due to the strong Coulomb interaction questions single-electron concepts like band structure or Fermi surface. Still, in practice these work surprisingly well. In fact, we can at least retain a nearly-independent-particle picture if we consider quasiparticles instead of electrons (or holes). In the case of electron injection into a sample the repulsive Coulomb interaction creates a Coulomb hole around the additional electron (see Figure 3). Analogously, if an electron leaves the system, its Coulomb hole also disappears. Relative to the ground-state N-electron system, the addition (removal) of an electron in indirect (direct) photoelectron spectroscopy hence creates (annihilates) an ensemble consisting of the bare electron and its oppositely charged Coulomb hole. This ensemble behaves in many ways like a single-particle and is thus called "quasiparticle". Since the Coulomb hole reduces the total charge of the quasiparticle, the effective interaction between quasiparticles is screened and considerably weaker than the bare Coulomb interaction between electrons. In fact, the screened interaction is sufficiently small so that the quasiparticles can be regarded as approximately independent, which finally justifies the independent-particle approximation and explains the success of mean-field theories.

A theoretical description of processes involving the ejection or injection of electrons requires a framework that links the N-particle with the $(N \pm 1)$-particle systems. For this purpose we employ many-body perturbation theory. The central variable is the time-ordered Green function $G(\mathbf{r}t, \mathbf{r}'t')$. As we will see, it contains the excitation energies ϵ_i and even the excitation lifetimes. Besides, we can directly obtain the ground-state electron density, the expectation values of one-particle operators and the ground-state total energy

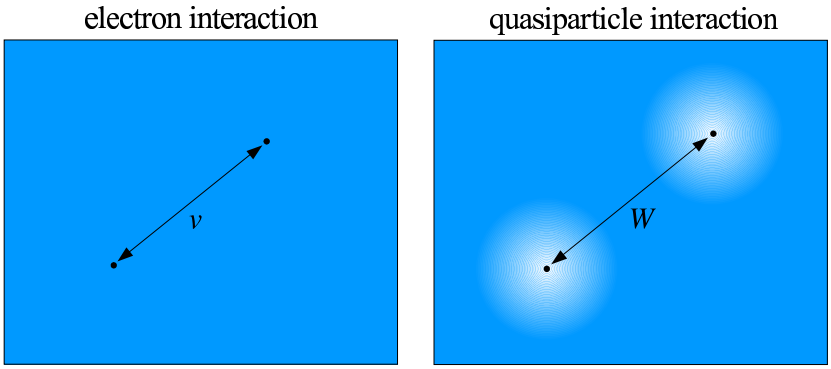

Figure 3. The electrons in a many-electron system are correlated by the strong Coulomb interaction v. The motion of one electron depends on the motion of all other electrons. A nearly-independent-particle picture can be recovered within the quasiparticle concept. Due to exchange and correlation effects a Coulomb hole forms around an electron and behaves together with it like a single entity, which is called quasiparticle. Quasiparticles interact via a weak screened interaction W instead of the strong Coulomb interaction.

from it. The Green function is hence capable of giving access to the same observables as the ground-state electron density. In contrast to the DFT expression $E[n]$, the functional $E[G]$ is even known exactly.[2] While the Green function contains much more information than the electron density, it is also a more complicated function and thus rarely applied to ground-state properties. In the present lecture we will, therefore, concentrate on the calculation of excited states.

Section 2 lays the theoretical foundations of the method. More complicated derivations are deferred to the appendix. The GW approximation is discussed in Section 3.1, and some aspects of its numerical implementation are given in Section 3.2. As an illustration, Section 3.3 presents a number of selected applications. Section 4 contains the summary.

2 Theory

2.1 Green Function

In this section we introduce the time-ordered Green function and examine its properties. We use the second-quantization formulation of quantum mechanics.[2,3] For the present purpose it is sufficient to know that this formalism involves field operators $\hat{\psi}(\mathbf{r})$ and $\hat{\psi}^\dagger(\mathbf{r})$ that describe the annihilation and the creation of an electron at the position $\mathbf{r}$, respectively. We will not take spin dependence explicitly into account. If necessary, the spin quantum number can simply be added to the formulas by considering it to be part of the spatial coordinate $\mathbf{r}$.

The Green function $G^{\mathrm{e}}(\mathbf{r}t, \mathbf{r}'t')$ is defined such that $i\hbar G^{\mathrm{e}}(\mathbf{r}t, \mathbf{r}'t')$ is the probability amplitude for the propagation of an additional electron from $(\mathbf{r}', t')$ to $(\mathbf{r}, t)$ in a many-electron system with the Hamiltonian (Eq. 41)). This process brings the system from the N-electron ground state $\left|\Psi_0^N(t')\right\rangle$ to a final state $\hat{\psi}(\mathbf{r})U(t,t')\hat{\psi}^\dagger(\mathbf{r}')\left|\Psi_0^N(t')\right\rangle$. The final state is constructed by the successive action of the electron creation operator $\hat{\psi}^\dagger(\mathbf{r}')$, the evolution operator $\hat{U}(t,t') = \exp[-i\hat{H}(t-t')/\hbar]$, which takes the system from t' to a later

time $t > t'$, and the electron annihilation operator $\hat{\psi}(\mathbf{r})$ on the N-electron ground state. As the probability amplitude is given by the overlap of the final state with $\left|\Psi_0^N(t)\right\rangle$, the Green function becomes

$$\begin{aligned} G^{\mathrm{e}}(\mathbf{r}t,\mathbf{r}'t') &= -\frac{i}{\hbar}\left\langle \Psi_0^N(t)\left|\hat{\psi}(\mathbf{r})\hat{U}(t,t')\hat{\psi}^\dagger(\mathbf{r}')\right|\Psi_0^N(t')\right\rangle\theta(t-t') \\ &= -\frac{i}{\hbar}\left\langle \Psi_0^N\left|\hat{\psi}(\mathbf{r}t)\hat{\psi}^\dagger(\mathbf{r}'t')\right|\Psi_0^N\right\rangle\theta(t-t')\,, \end{aligned} \tag{1}$$

where $\theta(t-t')$ is the Heaviside step function defined by

$$\theta(t-t') = \begin{cases} 1 \text{ if } t > t'\,, \\ 0 \text{ if } t < t'\,. \end{cases} \tag{2}$$

For the last equality in Eq. (1) we changed from the Schrödinger to the Heisenberg picture, where the expression is particularly simple. States and operators in the two pictures are related by

$$|\Psi_{\mathrm{H}}\rangle = \hat{U}(0,t)\,|\Psi_{\mathrm{S}}(t)\rangle \quad \text{and} \quad \hat{A}_{\mathrm{H}}(t) = \hat{U}(0,t)\hat{A}_{\mathrm{S}}\hat{U}(t,0)\,. \tag{3}$$

In the following we always omit the indices S and H. Similarly, we have the Green function

$$G^{\mathrm{h}}(\mathbf{r}'t',\mathbf{r}t) = -\frac{i}{\hbar}\left\langle \Psi_0^N\left|\hat{\psi}^\dagger(\mathbf{r}'t')\hat{\psi}(\mathbf{r}t)\right|\Psi_0^N\right\rangle\theta(t'-t) \tag{4}$$

for the propagation of an additional hole from $(\mathbf{r},t)$ to $(\mathbf{r}',t')$. As a matter of convenience, we combine the two expressions in one time-ordered Green function

$$G(\mathbf{r}t,\mathbf{r}'t') = G^{\mathrm{e}}(\mathbf{r}t,\mathbf{r}'t') - G^{\mathrm{h}}(\mathbf{r}'t',\mathbf{r}t) = -\frac{i}{\hbar}\left\langle \Psi_0^N\left|\hat{T}\left[\hat{\psi}(\mathbf{r}t)\hat{\psi}^\dagger(\mathbf{r}'t')\right]\right|\Psi_0^N\right\rangle\,, \tag{5}$$

where we used the time-ordering operator $\hat{T}$, which rearranges a series of field operators in order of ascending time arguments from right to left with a factor (-1) for each pair permutation. Depending on the time order, Eq. (5) describes either electron ($t > t'$) or hole ($t < t'$) propagation. The electron density $n(\mathbf{r})$ can be expressed in terms of the Green function as

$$n(\mathbf{r}t) = \left\langle \Psi_0^N\left|\hat{\psi}^\dagger(\mathbf{r}t)\hat{\psi}(\mathbf{r}t)\right|\Psi_0^N\right\rangle = -i\hbar G(\mathbf{r}t,\mathbf{r}t+\eta)\,. \tag{6}$$

Here and in the following η is an infinitesimal positive number. It serves only to enforce the correct order of the field operators. Its unit should always be clear from the context; presently it is an infinitesimal time.

Let us consider the time-ordered Green function $G(\mathbf{r},\mathbf{r}';\tau)$ of a stationary system with $\tau = t - t'$. If we insert the closure relation $\sum_i \left|\Psi_i^{N\pm1}\right\rangle\left\langle\Psi_i^{N\pm1}\right| = 1$ between the two field operators in Eq. (5), where $\left\{\left|\Psi_i^{N\pm1}\right\rangle\right\}$ is the complete set of state vectors of the $(N\pm1)$-particle system, transform to the Schrödinger picture and use the definitions

$$\psi_i^{N-1}(\mathbf{r}) = \left\langle \Psi_i^{N-1}\left|\hat{\psi}(\mathbf{r})\right|\Psi_0^N\right\rangle \quad \text{and} \quad \psi_i^{N+1}(\mathbf{r}) = \left\langle \Psi_0^N\left|\hat{\psi}(\mathbf{r})\right|\Psi_i^{N+1}\right\rangle \tag{7}$$

together with the excitation energies

$$\epsilon_i^{N-1} = E_0^N - E_i^{N-1} \quad \text{and} \quad \epsilon_i^{N+1} = E_i^{N+1} - E_0^N\,, \tag{8}$$

then we obtain

$$G(\mathbf{r},\mathbf{r}';\tau) = -\frac{i}{\hbar}\sum_i \psi_i^{N+1}(\mathbf{r})\psi_i^{N+1\,*}(\mathbf{r}')e^{-i\epsilon_i^{N+1}\tau/\hbar}\theta(\tau) + \frac{i}{\hbar}\sum_i \psi_i^{N-1}(\mathbf{r})\psi_i^{N-1\,*}(\mathbf{r}')e^{-i\epsilon_i^{N-1}\tau/\hbar}\theta(-\tau)\,. \tag{9}$$

The sums run over the ground state and all excited states of the $(N-1)$- and $(N+1)$-particle system, respectively. Expression (Eq. (9)) can be interpreted as follows: The state after the addition of an electron ($\tau > 0$) is represented by a linear combination of excited states

$$\hat{\psi}^\dagger(\mathbf{r}')\left|\Psi_0^N\right\rangle = \sum_i \psi_i^{N+1\,*}(\mathbf{r}')\left|\Psi_i^{N+1}\right\rangle \tag{10}$$

that subsequently evolve according to their respective phase factors $\exp(-i\epsilon_i^{N+1}\tau/\hbar)$. The resulting state is then probed at the point $\mathbf{r}$ by the projections $\psi_i^{N+1}(\mathbf{r})$. The case $\tau < 0$ (hole propagation) is analogous. Consequently, the Green function indeed contains the complete excitation spectrum of the $(N \pm 1)$-particle system. Fourier transformation of Eq. (9) to the frequency axis using the Fourier transform of the Heaviside step function

$$\theta(\omega) = \frac{1}{2\pi}\int_{-\infty}^{\infty}\theta(\tau)\; e^{i\omega\tau-\eta|\tau|}d\tau = \frac{i}{2\pi\,(\omega+i\eta)} \tag{11}$$

finally yields the Lehmann representation of the Green function

$$G(\mathbf{r}',\mathbf{r};\omega) = \sum_i \frac{\psi_i^{N+1}(\mathbf{r})\psi_i^{N+1\,*}(\mathbf{r})}{\hbar\omega-\epsilon_i^{N+1}+i\eta} + \sum_i \frac{\psi_i^{N-1}(\mathbf{r})\psi_i^{N+1\,*}(\mathbf{r})}{\hbar\omega-\epsilon_i^{N-1}-i\eta}\,. \tag{12}$$

We observe that the Green function has poles at the true many-particle excitation energies $\epsilon_i^{N\pm1}$. These energies correspond to excitations of an $(N-1)$-particle and an $(N+1)$-particle system and hence to those processes measured in direct and inverse photoelectron spectroscopy. In the case of a noninteracting (or mean-field) system the $\psi_i^{N+1}(\mathbf{r})$ are simply the unoccupied and the $\psi_i^{N-1}(\mathbf{r})$ the occupied single-particle wave functions, the $\epsilon_i^{N\pm1}$ are the corresponding single-particle energies. In order not to overload the notation, we will drop the $(N \pm 1)$ superscripts from now on.

2.2 Spectral Function

In connection with Eq. (9) we can define the spectral function $A(\mathbf{r},\mathbf{r}';\omega)$, i.e., the density of the excited (or quasiparticle) states that contribute to the electron or hole propagation. In a finite system this density is a series of delta functions at the excitation energies

$$A(\mathbf{r},\mathbf{r}';\omega) = \sum_i \psi_i(\mathbf{r})\psi_i^*(\mathbf{r}')\delta(\hbar\omega-\epsilon_i) \tag{13}$$

weighted by the products of the corresponding projections (Eq. (7)). This allows us to rewrite Eq. (12) as an integral over frequencies

$$G(\mathbf{r},\mathbf{r}';\omega) = \hbar\int_{-\infty}^{\infty}\frac{A(\mathbf{r},\mathbf{r}';\omega')}{\hbar\omega-\hbar\omega'+\mathrm{sgn}(\hbar\omega'-\mu)\,i\eta}d\omega' \tag{14}$$

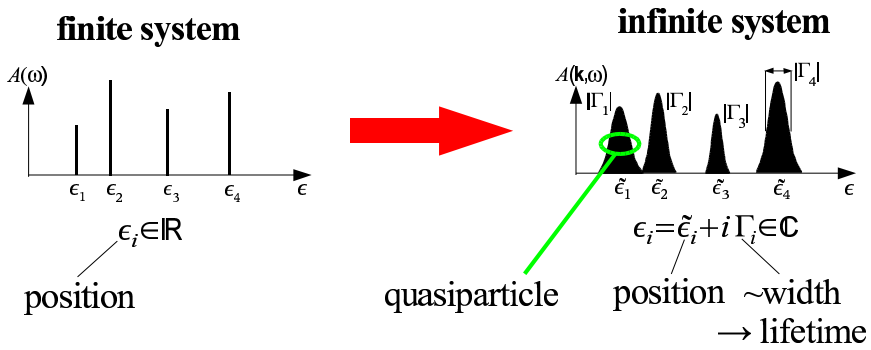

Figure 4. The excitation peaks of a finite system in the spectral function $A(\omega)$ merge into quasiparticle peaks of finite width in the case of an infinite system. This gives rise to finite excitation lifetimes determined by the inverse of the peak widths.

with $\max\left(\epsilon_i^{N-1}\right) \leq \mu \leq \min\left(\epsilon_i^{N+1}\right)$. In an infinite system μ corresponds to the chemical potential. The inequality $\max\left(\epsilon_i^{N-1}\right) \leq \min\left(\epsilon_i^{N+1}\right)$ follows from the convexity of the total energy as a function of the particle number, i.e., $E_0^{N-1} - E_0^N \geq E_0^N - E_0^{N+1}$: we lose more energy when removing an electron than we gain by adding one. With the identity

$$\frac{1}{x \mp i\eta} = \mathcal{P}\left(\frac{1}{x}\right) \pm i\pi\delta(x) \tag{15}$$

in the limit $\eta \to 0^+$, where $\mathcal{P}(1/x)$ is the principal value of $1/x$, we find that

$$A(\mathbf{r}, \mathbf{r}'; \omega) = -\mathrm{sgn}(\hbar\omega - \mu)\, \frac{1}{\pi}\, \mathrm{Im}\, G(\mathbf{r}, \mathbf{r}'; \omega)\,. \tag{16}$$

The closure relation of the functions in Eq. (7) yields another important property

$$\hbar \int_{-\infty}^{\infty} A(\mathbf{r}, \mathbf{r}'; \omega) d\omega = \sum_i \psi_i(\mathbf{r}) \psi_i^*(\mathbf{r}') = \delta(\mathbf{r} - \mathbf{r}')\,. \tag{17}$$

When we change from a finite to an infinite system, the delta functions in $A(\mathbf{r}, \mathbf{r}'; \omega)$ merge and form a series of smooth peaks with finite line widths instead of sharp resonances (see Figure 4). However, if the resulting spectral features are of Lorentzian form, i.e.,

$$A(\mathbf{r}, \mathbf{r}'; \omega) = \sum_i \psi_i(\mathbf{r}) \psi_i^*(\mathbf{r}') \frac{\Gamma_i}{\left(\hbar\omega - \tilde{\epsilon}_i\right)^2 + \Gamma_i^2}\,, \tag{18}$$

where the $\tilde{\epsilon}_i$ are the peak positions and $|\Gamma_i|$ the corresponding peak widths, then we can perform the integration in Eq. (14) analytically and again obtain a discrete sum over i as in Eq. (12), provided that the energies are defined as complex numbers $\epsilon_i = \tilde{\epsilon}_i + i\Gamma_i$. Consequently, the form of the Fourier transform (Eq. (9)) remains unchanged, too. The imaginary component of ϵ_i leads to a damping term $\exp(-|\Gamma_i \tau|/\hbar)$, revealing that the excitation has a finite lifetime of $\hbar\,|\Gamma_i|^{-1}$. Physically, the de-excitation proceeds via Auger transitions that create electron-hole pairs on the way. The damping of the particle propagator G may seem surprising, as it suggests that the particle gradually disappears. However, one must keep in mind that we deal with an infinite system, i.e., $N \to \infty$, and an additional particle

(electron or hole) can "dissipate" into the Fermi sea. In this sense, one often speaks of finite quasiparticle lifetimes and calls $\psi_i(\mathbf{r})$ and ϵ_i the quasiparticle wave functions and energies, respectively. The quasiparticle equation (22) introduced in the next section holds for infinite systems if one uses an analytic continuation of the self-energy into the complex frequency plane.

2.3 Dyson Equation

Appendix A shows that the time-ordered Green function $G(\mathbf{r}, \mathbf{r}'; \omega)$ of the interacting system obeys an integral equation, the Dyson equation

$$G(\mathbf{r}, \mathbf{r}'; \omega) = G_0(\mathbf{r}, \mathbf{r}'; \omega) + \iint G_0(\mathbf{r}, \mathbf{r}''; \omega)\Sigma(\mathbf{r}'', \mathbf{r}'''; \omega)G(\mathbf{r}''', \mathbf{r}'; \omega)d^3r''d^3r''' \,, \quad (19)$$

where $G_0(\mathbf{r}, \mathbf{r}'; \omega)$ is the Green function of a mean-field system defined by

$$\hat{h}_0\varphi_i^0(\mathbf{r}) = \epsilon_i^0\varphi_i^0(\mathbf{r}) \quad (20)$$

with the single-particle Hamiltonian

$$\hat{h}_0(\mathbf{r}) = -\frac{\hbar^2}{2m}\nabla^2 + V_{\rm ext}(\mathbf{r}) + \frac{e^2}{4\pi\varepsilon_0}\int \frac{n(\mathbf{r}')}{|\mathbf{r} - \mathbf{r}'|}d^3r' \,. \quad (21)$$

The quantities $V_{\rm ext}(\mathbf{r})$, m, e and ε_0 are defined as in Eq. (41). The Green function $G_0(\mathbf{r}, \mathbf{r}'; \omega)$ is obtained from Eq. (12) with the wave functions $\varphi_i^0(\mathbf{r})$ and energies ϵ_i^0. The nonlocal and frequency-dependent function $\Sigma(\mathbf{r}, \mathbf{r}', \omega)$ is the non-Hermitian self-energy operator, which contains all many-body exchange and correlation effects beyond the electrostatic Hartree potential. This can be more easily seen in a reformulation of the Dyson equation. By inserting the Lehmann representation (Eq. (12)) into Eq. (19), we find that the wave functions $\psi_i(\mathbf{r})$ and energies ϵ_i obey the quasiparticle equation

$$\hat{h}_0(\mathbf{r})\psi_i(\mathbf{r}) + \int \Sigma(\mathbf{r}, \mathbf{r}'; \epsilon_i/\hbar)\psi_i(\mathbf{r}')d^3r' = \epsilon_i\psi_i(\mathbf{r}) \quad (22)$$

(see Appendix B), which is nonlinear in ϵ_i. Although it looks very similar to the one-particle equations of mean-field approaches like Hartree, Hartree-Fock or DFT, it does *not* constitute a mean-field formulation, since the self-energy takes all dynamic many-electron processes into account. Consequently, the functions $\psi_i(\mathbf{r})$ and energies ϵ_i must not be understood as single-particle quantities. In fact, they are defined in Eqs. (7) and (8) as properties of the many-electron system. From the nonlinearity of the quasiparticle equation it follows that the wave functions $\psi_i(\mathbf{r})$ are not orthonormal, in contrast to single-particle wave functions. However, they do fulfill the closure relation (Eq. (17)).

The Dyson equation (19) can be rewritten in the form of a geometric series by subsequently replacing G on the right-hand side by $G_0 + G_0\Sigma G$, which leads to, symbolically written,

$$G = G_0 + G_0\Sigma G_0 + G_0\Sigma G_0\Sigma G_0 + G_0\Sigma G_0\Sigma G_0\Sigma G_0 + \ldots \,. \quad (23)$$

This is a typical equation of scattering theory, where the different terms of the geometric series describe single, double, triple, etc., scattering processes, and Σ is the scattering potential. Such a succession of scattering processes can be illustrated by Feynman diagrams,

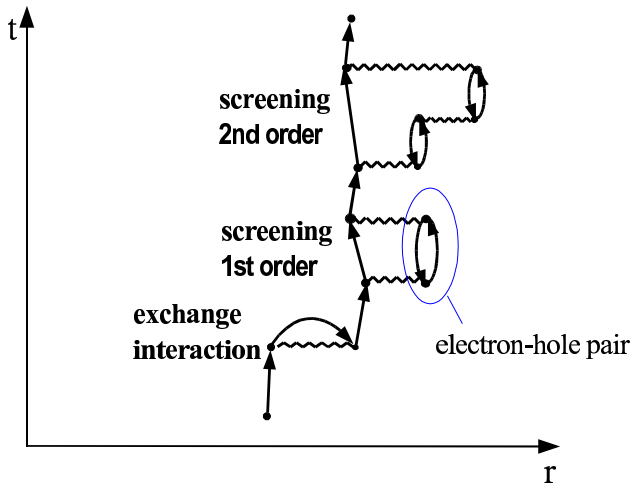

Figure 5. Illustration of a series of scattering processes using Feynman diagrams. All zigzag lines representing the instantaneous Coulomb interaction must be drawn horizontally. Arrows going forward in time represent electron and those going backward in time hole propagators. The self-energy is the sum of all possible single scattering processes.

where G_0 is drawn as a straight arrow and the Coulomb interaction as a zigzag line. According to Eq. (23), a diagrammatic representation of a multiple scattering process should involve a series of arrows (G_0) divided by single scattering processes (Σ). In the example of Figure 5 these are the exchange interaction, the creation of an electron-hole pair (the "bubble" diagram) and finally the creation of a pair that itself creates another pair. In order to obtain the complete Green function, we have to sum all multiple scattering processes, of which the one shown in Figure 5 is merely one example. The self-energy is given by the sum of all single scattering processes. The interpretation in terms of scattering processes allows to construct approximations for Σ by the summation of diagrams considered essential for the physical behavior of a given electron system. In general, however, such approximations are rarely convergent, and too many processes turn out to be quantitatively important. Therefore, we apply a systematic algebraic method instead.

3 Implementation and Applications

3.1 *GW* Approximation

In practice we must use an approximation for the self-energy, such as the GW approximation, which contains the electron exchange and a large part of the electron correlation. It is formally derived in Appendix A and has a very simple mathematical form in the time domain

$$\Sigma^{GW}(\mathbf{r},\mathbf{r}';\tau) = i\hbar G_0(\mathbf{r},\mathbf{r}';\tau)W(\mathbf{r},\mathbf{r}';\tau+\eta)\,. \tag{24}$$

In order to calculate the self-energy contribution to the quasiparticle energies, we need the Fourier transform on the frequency axis

$$\Sigma^{GW}(\mathbf{r},\mathbf{r}';\omega) = \frac{i\hbar}{2\pi}\int_{-\infty}^{\infty} G_0(\mathbf{r},\mathbf{r}';\omega+\omega')W(\mathbf{r},\mathbf{r}';\omega')e^{i\omega'\eta}d\omega' \,. \tag{25}$$

The first function on the right-hand side is the Green function of the noninteracting system defined by Eq. (20) and the second function the dynamically screened interaction $W(\mathbf{r},\mathbf{r}';\omega)$, which is related to the bare Coulomb potential $v(\mathbf{r},\mathbf{r}') = e^2/\left(4\pi\varepsilon_0\left|\mathbf{r}-\mathbf{r}'\right|\right)$ through the inverse of the dielectric function

$$W(\mathbf{r},\mathbf{r}';\omega) = \int \varepsilon^{-1}(\mathbf{r},\mathbf{r}'';\omega)v(\mathbf{r}'',\mathbf{r}')d^3r'' = v(\mathbf{r},\mathbf{r}') + \int n_{\mathrm{ind}}(\mathbf{r},\mathbf{r}'';\omega)v(\mathbf{r}'',\mathbf{r}')d^3r'' \,. \tag{26}$$

The screened interaction $W(\mathbf{r},\mathbf{r}';\omega)$ is the effective potential at $\mathbf{r}'$ induced by a quasiparticle at $\mathbf{r}$: the Coulomb potential of the electron repels other electrons in its neighborhood and thus gives rise to the formation of an exchange and correlation hole, whose effective positive charge $n_{\mathrm{ind}}(\mathbf{r},\mathbf{r}'';\omega)$ screens the bare Coulomb potential $v(\mathbf{r},\mathbf{r}')$ (see Figure 6). Analogously, an effective negative charge screens the Coulomb potential of a hole. The screened interaction is considerably weaker than the bare Coulomb interaction. The GW approximation uses the random-phase approximation (RPA)

$$\varepsilon(\mathbf{r},\mathbf{r}';\omega) = \delta(\mathbf{r}-\mathbf{r}') - \int v(\mathbf{r},\mathbf{r}'')P(\mathbf{r}'',\mathbf{r}';\omega)d^3r'' \,, \tag{27}$$

$$P(\mathbf{r},\mathbf{r}';\tau) = -i\hbar G_0(\mathbf{r},\mathbf{r}';\tau)G_0(\mathbf{r}',\mathbf{r};-\tau) \,. \tag{28}$$

It corresponds to a subset of scattering processes in the many-electron system. Some of the respective diagrams are just the ones shown in Figure 5. Using expression in Eq. (12) for the Green function G_0 of the noninteracting system we observe that the Fourier transform of the polarization function in Eq. (28) is given by

$$P\left(\mathbf{r},\mathbf{r}';\omega\right) = \sum_{i}^{\text{occ.}}\sum_{j}^{\text{unocc.}} \varphi_i^0\left(\mathbf{r}\right)\varphi_j^{0*}\left(\mathbf{r}\right)\varphi_i^{0*}\left(\mathbf{r}'\right)\varphi_j^0\left(\mathbf{r}'\right) \times\left(\frac{1}{\hbar\omega+\epsilon_i^0-\epsilon_j^0+i\eta}-\frac{1}{\hbar\omega-\epsilon_i^0+\epsilon_j^0-i\eta}\right) \tag{29}$$

in terms of the wave functions $\varphi_i^0(\mathbf{r})$ and energies ϵ_i^0.

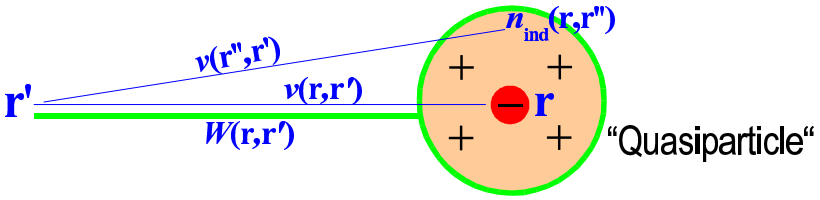

Figure 6. The formation of the Coulomb hole around an electron at $\mathbf{r}$ screens its Coulomb potential $v(\mathbf{r},\mathbf{r}')$. This leads to the definition of the screened interaction $W(\mathbf{r},\mathbf{r}')$ that takes into account the combined potentials of the bare electron and its screening cloud n_{ind}. The ensemble consisting of the electron and its polarization cloud is called "quasiparticle".

The well-known Hartree-Fock equations can be recovered from Eq. (22) if we use the energy-independent self-energy

$$\Sigma^{\mathrm{HF}}(\mathbf{r},\mathbf{r}') = i\hbar G_0(\mathbf{r},\mathbf{r}';-\eta)v(\mathbf{r},\mathbf{r}') \tag{30}$$

(given in the time domain) instead. By comparison with Eq. (24), we see that the GW approximation constitutes an expansion of the self-energy up to first order in the screened interaction as opposed to the bare Coulomb interaction in Eq. (30). This approximates the exact self-energy considerably better, because W is much smaller than v. Due to the similarity of the two self-energy expressions, the GW approximation can formally be regarded as a Hartree-Fock approach with a dynamically screened interaction W instead of the static Coulomb interaction v.

3.2 Numerical Implementation

For band structure calculations it is more efficient to obtain the ϵ_i directly from the quasiparticle equation (22) instead of solving the Dyson integral equation (19) and searching for the poles of the Green function. Furthermore, it is then possible to exploit the formal similarity to the Kohn-Sham equation

$$\hat{h}_0\varphi_i^{\mathrm{KS}}(\mathbf{r}) + V_{\mathrm{xc}}(\mathbf{r})\varphi_i^{\mathrm{KS}}(\mathbf{r}) = \epsilon_i^{\mathrm{KS}}\varphi_i^{\mathrm{KS}}(\mathbf{r})\,, \tag{31}$$

where $V_{\mathrm{xc}}(\mathbf{r})$ is the local exchange-correlation potential. In many cases the Kohn-Sham eigenvalues ϵ_i^{KS} already provide a reasonable estimate of the band structure and are in qualitative agreement with experiment. For systems where the quasiparticle wave functions are known, one also finds $\varphi_i^{\mathrm{KS}}(\mathbf{r}) \approx \psi_i(\mathbf{r})$.[9] This observation indicates that the self-energy correction $\Sigma\left(\mathbf{r},\mathbf{r}';\epsilon_i/\hbar\right) - V_{\mathrm{xc}}(\mathbf{r})\delta(\mathbf{r}-\mathbf{r}')$ is small and justifies the use of first-order perturbation theory to obtain approximate energies

$$\epsilon_i \approx \epsilon_i^{\mathrm{KS}} + \left\langle \varphi_i^{\mathrm{KS}} \left| \Sigma\left(\epsilon_i/\hbar\right) - V_{\mathrm{xc}} \right| \varphi_i^{\mathrm{KS}} \right\rangle\,. \tag{32}$$

A solution of this nonlinear equation still requires the knowledge of the frequency dependence of the self-energy, which is not known in general. Therefore, we use the linear expansion

$$\Sigma(\mathbf{r},\mathbf{r}';\epsilon_i/\hbar) \approx \Sigma(\mathbf{r},\mathbf{r}';\epsilon_i^{\mathrm{KS}}/\hbar) + \frac{\epsilon_i-\epsilon_i^{\mathrm{KS}}}{\hbar}\frac{\partial\Sigma(\mathbf{r},\mathbf{r}';\epsilon_i^{\mathrm{KS}}/\hbar)}{\partial\omega}\,, \tag{33}$$

which leads to

$$\epsilon_i \approx \epsilon_i^{\mathrm{KS}} + Z_i\left\langle \varphi_i^{\mathrm{KS}} \left| \Sigma\left(\epsilon_i^{\mathrm{KS}}/\hbar\right) - V_{\mathrm{xc}} \right| \varphi_i^{\mathrm{KS}} \right\rangle\,. \tag{34}$$

The quasiparticle renormalization factor is given by

$$Z_i = \left(1 - \left\langle \varphi_i^{\mathrm{KS}} \left| \frac{1}{\hbar}\frac{\partial\Sigma\left(\epsilon_i^{\mathrm{KS}}/\hbar\right)}{\partial\omega} \right| \varphi_i^{\mathrm{KS}} \right\rangle\right)^{-1} \tag{35}$$

and equals the quasiparticle weight

$$Z_i = \int \left|\psi_i(\mathbf{r})\right|^2 d^3r < 1\,. \tag{36}$$

With the decomposition of W into the bare Coulomb interaction v and the remainder $W - v$, the GW self-energy (Eq. (24)) splits into exchange and correlation parts, symbolically written as

$$\Sigma^{GW} = i\hbar G_0^{\mathrm{KS}} W = i\hbar G_0^{\mathrm{KS}} v + i\hbar G_0^{\mathrm{KS}} (W - v) = \Sigma_{\mathrm{x}}^{GW} + \Sigma_{\mathrm{c}}^{GW} \,. \tag{37}$$

Instead of G_0 we use the Kohn-Sham Green function G_0^{KS}. After inserting this decomposition into Eq. (25), we must evaluate the convolutions

$$\Sigma_{\mathrm{x}}^{GW}(\mathbf{r}, \mathbf{r}'; \omega) = \frac{i\hbar}{2\pi} \int_{-\infty}^{\infty} G_0^{\mathrm{KS}}(\mathbf{r}, \mathbf{r}'; \omega + \omega') v(\mathbf{r}, \mathbf{r}') e^{i\omega'\eta} d\omega' \,, \tag{38a}$$

$$\Sigma_{\mathrm{c}}^{GW}(\mathbf{r}, \mathbf{r}'; \omega) = \frac{i\hbar}{2\pi} \int_{-\infty}^{\infty} G_0^{\mathrm{KS}}(\mathbf{r}, \mathbf{r}'; \omega + \omega') \left[W(\mathbf{r}, \mathbf{r}'; \omega') - v(\mathbf{r}, \mathbf{r}') \right] d\omega' \,. \tag{38b}$$

The integral (Eq. (38a)) can be evaluated analytically and leads to the well-known expression for the Hartree-Fock exchange term

$$\left\langle \varphi_i^{\mathrm{KS}} \left| \Sigma_{\mathrm{x}}^{GW} \right| \varphi_i^{\mathrm{KS}} \right\rangle = -\frac{e^2}{4\pi\varepsilon_0} \sum_j^{\mathrm{occ.}} \int \frac{\varphi_i^{\mathrm{KS}\,*}(\mathbf{r})\, \varphi_j^{\mathrm{KS}}(\mathbf{r})\, \varphi_j^{\mathrm{KS}\,*}(\mathbf{r}')\, \varphi_i^{\mathrm{KS}}(\mathbf{r}')}{|\mathbf{r} - \mathbf{r}'|} d^3r\, d^3r' \,. \tag{39}$$

In general, the second convolution (Eq. (38b)) must be computed numerically. For this purpose the integration contour is usually deformed to the complex plane, where the analytical continuations of G_0 and W are smoother.

Let the Kohn-Sham wave functions be represented in a basis $\{\zeta_\alpha(\mathbf{r})\}$. According to Eq. (29) we can then write the polarization function and all related quantities in terms of products $\chi_\mu(\mathbf{r}) = \zeta_\alpha^*(\mathbf{r})\zeta_\beta(\mathbf{r})$ with the composite index $\mu = (\alpha, \beta)$ as

$$P(\mathbf{r}, \mathbf{r}'; \omega) = \sum_{\mu,\nu} P_{\mu\nu}(\omega) \chi_\mu^*(\mathbf{r}) \chi_\nu(\mathbf{r}') \,. \tag{40}$$

The Eqs. (24) to (28) are solved by matrix operations:

1. A self-consistent DFT loop produces the Kohn-Sham wave functions $\varphi_i^{\mathrm{KS}}(\mathbf{r})$ and energies ϵ_i^{KS}. At this point we can already evaluate the exchange term (Eq. (39)).
2. The polarization matrix $P_{\mu\nu}(\omega)$ is calculated according to Eq. (29).
3. The dielectric matrix is obtained from $\varepsilon_{\mu\nu}(\omega) = \delta_{\mu\nu} - \sum_\gamma v_{\mu\gamma} P_{\gamma\nu}(\omega)$ and inverted.
4. Next the screened interaction $W_{\mu\nu}(\omega) = \sum_\gamma \varepsilon_{\mu\gamma}^{-1}(\omega) v_{\gamma\nu}$ is calculated from a matrix multiplication of the inverse dielectric function with the Coulomb matrix.
5. The correlation term $\left\langle \varphi_i^{\mathrm{KS}} \left| \Sigma_{\mathrm{c}}^{GW} \right| \varphi_i^{\mathrm{KS}} \right\rangle$ is evaluated according to Eq. (38b) with a numerical contour integration on the complex frequency plane.
6. Finally, approximate quasiparticle energies are obtained from Eqs. (34) and (35).

The computation of the dielectric function, its inversion and the convolution (Eq. (38b)) are very time-consuming. Therefore, some (especially older) codes approximate the inverse dielectric function by a so-called plasmon-pole model.[10,11] These models replace the imaginary component of $\varepsilon^{-1}(\omega)$, which has a peaked structure, by a sum of delta functions

at the corresponding frequencies. This simplification reduces the third step to a single matrix inversion of the static dielectric function at $\omega = 0$ and makes an analytic evaluation of the frequency integral (Eq. (38b)) possible.

3.3 Examples

Although Hedin's seminal article[4] was already published in 1965, it was not before the middle of the 1980s that the first ab initio calculations for real materials were reported in the literature. In spite of several approximations in the numerical treatment, which were necessary because of the lack of computer power back then, initial results were already very promising. Hybertsen and Louie[12] as well as Godby *et al.*[13] showed that the calculated band gap of Si fell within a margin of about 0.1 eV from the experimental value. Shortly afterwards the same authors reported band gaps for several other semiconducting materials that turned out to be equally accurate.[14,15] After these pioneering studies the GW approximation was applied to a variety of semiconductors with great success (see, e.g., Figure 1). The principal effect of the GW self-energy correction on the band structure of a semiconductor is to rigidly shift the valence bands up and the conduction bands down, thus opening the band gap. Figure 7 shows this effect for Si as an example.

Not only the band gaps of semiconductors and insulators are improved by the GW self-energy correction, but the correlation-induced band narrowing of metals is also correctly described. The band narrowing reflects the higher effective mass of quasiparticles (the polarization cloud adds to the electron mass) compared to bare electrons. For this reason, the self-energy is sometimes also referred to as "mass operator". Figure 8 shows the energy

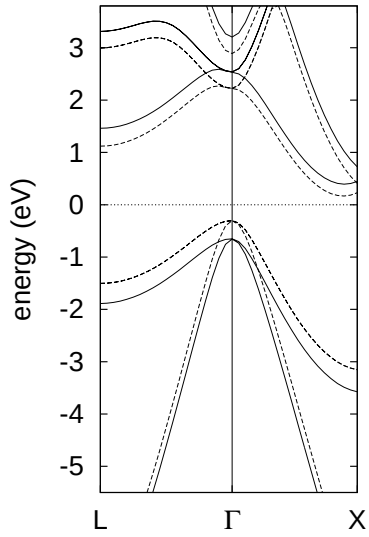

Figure 7. LDA band structure (dashed lines) of silicon with GW self-energy corrected valence and conduction bands (solid lines). The GW approximation shifts the corresponding bands up and down, respectively, but leaves the dispersion essentially unaffected.

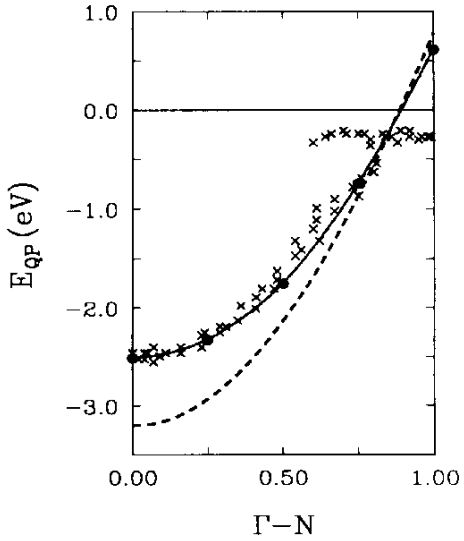

Figure 8. Comparison of LDA (dashed), quasiparticle (solid line) and experimental (crosses) bands for Na. Taken from Ref. 16.

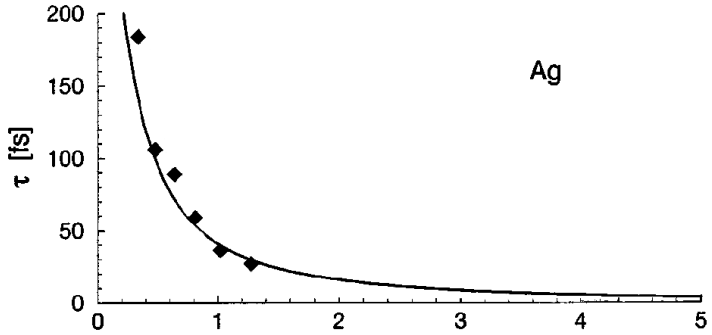

Figure 9. De-excitation dynamics measured in time-resolved two-photon photoemission spectroscopy (diamonds) and calculated with the *GW* approximation (solid line). Taken from Ref. 17.

dispersion of Na as an example.[16] The band narrowing brought about by the GW self-energy correction leads to nearly perfect agreement with experiment.

The calculated excitation or quasiparticle lifetimes can be directly compared with two-photon photoemission spectroscopy. This experimental method allows to measure dynamical de-excitation processes in electronic systems. After a first photon has excited the electron system (creating a "hot" electron), a second photon probes the quasiparticle density of states like in ordinary direct photoelectron spectroscopy. The time delay between the two photons can be tuned such that the system can be observed in different stages of the electronic de-excitation process. From a series of measurements one can thus deduce the

lifetime, which depends on the excitation energy, i.e., the energy of the first photon. In the example of Ag in Figure 9 the theoretical curve $\tau = \hbar\,|\Gamma|^{-1}$ obtained from the imaginary parts of the quasiparticle energies (see Section 2.2) closely follows the experimental data points.[17]

4 Summary

In this lecture we presented the GW approximation for the electronic self-energy, which allows to calculate excited-state properties like excitation energies and lifetimes. The self-energy describes scattering processes between electrons and, in principle, contains all exchange and correlation effects beyond the electrostatic Hartree potential. The GW approximation includes a subset of these scattering processes. Apart from exchange it describes the creation of electron-hole pairs within the random-phase approximation (RPA) that leads to the formation of polarization clouds around the bare particles. The ensemble of an electron or a hole together with its polarization cloud behaves essentially like a single entity and is called a quasiparticle. The quasiparticles interact via a screened potential that is considerably weaker than the bare Coulomb interaction. This makes a perturbative treatment possible. In this respect, the GW approximation constitutes an expansion of the self-energy up to linear order in the screened interaction. It works well in a large class of systems where the polarization effects covered by the RPA play the dominant role in electron correlation, such as simple metals and semiconductors.

The GW approximation is by nature a perturbative approach. Actual GW calculations are usually based on the self-consistent Kohn-Sham wave functions and energies as a starting point. This method has its limitations in materials where DFT already gives unphysical results. It breaks down for systems with very strong electronic correlation, which is insufficiently described by the available exchange-correlation functionals. The large error in the band gap of NiO in Figure 1 is an example. In reality, NiO is a strongly correlated Mott-Hubbard insulator, whereas it comes out as a semiconductor with a very small band gap (nearly a semi-metal) in DFT calculations.

The GW method is designed for the analysis of excited states of the $(N \pm 1)$-electron systems. The treatment of optical absorption processes, where the particle number does not change due to the promotion of valence electrons into unoccupied conduction states rather than emission, requires the simultaneous description of two particles, an electron and a hole, i.e., an exciton. Consequently, one must describe such a process with a two-particle Green function. In this case many-body perturbation theory leads to the so-called Bethe-Salpeter equation. Absorption spectra obtained from this equation are indeed very accurate.[18] An alternative is time-dependent density functional theory,[19] which also gives access to the excited states of an N-electron system.

Appendix A

Hedin equations

With the field-operators introduced in Section 2.1 we can rewrite the many-particle Hamiltonian

$$\hat{H} = \sum_i \left[-\frac{\hbar^2}{2m}\nabla_i^2 + V_{\text{ext}}(\mathbf{r}_i) \right] + \frac{1}{2}\sum_{ij} v(\mathbf{r}_i, \mathbf{r}_j)\,, \tag{41}$$

where $V_{\text{ext}}(\mathbf{r})$ is the potential created by the atomic nuclei, $v(\mathbf{r},\mathbf{r}') = e^2/\left(4\pi\varepsilon_0 \left|\mathbf{r}-\mathbf{r}'\right|\right)$ the Coulomb interaction, m the electron mass, e the electron charge and ε_0 the vacuum dielectric constant, as

$$\hat{H} = \int \hat{\psi}^\dagger(\mathbf{r})\hat{h}(\mathbf{r})\hat{\psi}(\mathbf{r})d^3r + \frac{1}{2}\iint \hat{\psi}^\dagger(\mathbf{r})\hat{\psi}^\dagger(\mathbf{r}')v(\mathbf{r},\mathbf{r}')\hat{\psi}(\mathbf{r}')\hat{\psi}(\mathbf{r})d^3r\, d^3r' \tag{42}$$

with the one-particle operator

$$\hat{h}(\mathbf{r}) = -\frac{\hbar^2}{2m}\nabla^2 + V_{\text{ext}}(\mathbf{r})\,. \tag{43}$$

The expression in Eq. (42) is just a mathematical reformulation of Eq. (41) and should not be mistaken for the energy expectation value in Hartree theory, although it looks similar.

From the equation of motion for the annihilation operator

$$i\hbar\frac{\partial}{\partial t}\hat{\psi}(\mathbf{r},t) = \left[\hat{\psi}(\mathbf{r},t), \hat{H}\right]_- = \hat{h}(\mathbf{r})\hat{\psi}(\mathbf{r},t) + \int v(\mathbf{r},\mathbf{r}')\hat{\psi}^\dagger(\mathbf{r}',t)\hat{\psi}(\mathbf{r}',t)\hat{\psi}(\mathbf{r},t)d^3r'\,, \tag{44}$$

which describes the time evolution of a Heisenberg operator in the same way as the Schrödinger equation describes that of a wave function, we can directly deduce the equation of motion for the Green function

$$\begin{aligned} i\hbar\frac{\partial}{\partial t}G(\mathbf{r}t,\mathbf{r}'t') &= \delta(\mathbf{r}-\mathbf{r}')\delta(t-t') + \hat{h}(\mathbf{r})G(\mathbf{r}t,\mathbf{r}'t') \\ &-\frac{i}{\hbar}\int v(\mathbf{r},\mathbf{r}'')\left\langle \Psi_0^N \left| \hat{T}\left[\hat{\psi}^\dagger(\mathbf{r}'',t)\hat{\psi}(\mathbf{r}'',t)\hat{\psi}(\mathbf{r},t)\hat{\psi}^\dagger(\mathbf{r}',t')\right]\right| \Psi_0^N \right\rangle d^3r''\,. \end{aligned} \tag{45}$$

This is not a closed equation, because it involves the two-particle Green function

$$G(1234) = -\frac{1}{\hbar^2}\left\langle \Psi_0^N \left| \hat{T}\left[\hat{\psi}(1)\hat{\psi}(2)\hat{\psi}^\dagger(4)\hat{\psi}^\dagger(3)\right]\right| \Psi_0^N \right\rangle\,. \tag{46}$$

Here and in the following we denote the set of space-time coordinates $(\mathbf{r}_1, t_1)$ with a natural number 1, etc., and further define

$$\delta(12) = \delta(\mathbf{r}_1-\mathbf{r}_2)\delta(t_1-t_2)\,, \tag{47}$$

$$v(12) = v(\mathbf{r}_1,\mathbf{r}_2)\delta(t_1-t_2)\,, \tag{48}$$

$$\int d1 = \int d^3r_1 \int_{-\infty}^{\infty} dt_1\,, \tag{49}$$

$$1^+ = (\mathbf{r}_1, t_1+\eta)\,, \tag{50}$$

where η is an infinitesimal positive time. With the two-particle Green function (Eq. (46)) we can rewrite Eq. (45) as

$$i\hbar\frac{\partial}{\partial t_1}G(12) = \delta(12) + \hat{h}(1)G(12) - i\hbar\int v(1^+3)G(1323^+)d3\,. \tag{51}$$

The additional infinitesimals in 1^+ and 3^+ make sure that the time order is the same as in Eq. (45).

In order to employ the functional-derivative method, we introduce an external potential $U(1)$ that is again set to zero at the end. Of course, all quantities from now on depend on $U(1)$, while the equations remain invariant provided that we replace $\hat{h}(1) \to \hat{h}(1) + U(1)$. We can use functional differentiation to define a number of useful quantities. The reaction of the density to changes in the external potential is governed by the linear-response function

$$R(12) = \left.\frac{\delta n(1)}{\delta U(2)}\right|_{U=0}\,. \tag{52}$$

The test potential and the Coulomb potential created by the induced charge can be combined into an effective potential

$$U_{\text{eff}}(1) = U(1) + \iint v(13)R(32)U(2)d2\,d3\,, \tag{53}$$

which is related to $U(1)$ via the inverse dielectric function

$$\varepsilon^{-1}(12) = \left.\frac{\delta U_{\text{eff}}(1)}{\delta U(2)}\right|_{U=0} = \delta(12) + \int v(13)R(32)d3\,. \tag{54}$$

With the definition of the polarization function

$$P(12) = \left.\frac{\partial n(1)}{\partial U_{\text{eff}}(2)}\right|_{U=0} \tag{55}$$

and the chain rule for functional derivatives one obtains the geometric series

$$\varepsilon^{-1}(12) = \delta(12) + \int v(13)P(32)d3 + \iiint v(13)P(34)v(45)P(52)d3\,d4\,d5 + \dots\,, \tag{56}$$

which can easily be inverted to yield

$$\varepsilon(12) = \delta(12) - \int v(13)P(32)d3\,. \tag{57}$$

If we take the Coulomb potential of an electron at 2 as the test potential, we get the screened potential

$$W(12) = \int \varepsilon^{-1}(13)v(32)d3 = v(12) + \iint v(13)P(34)W(42)d3\,d4 \tag{58}$$

as the effective potential at position 1.

After this interlude we can go on with the derivation. For the functional derivative of the Green function with respect to the test potential we find[4,20]

$$\left.\frac{\delta G(12)}{\delta U(3)}\right|_{U=0} = G(12)G(33^+) - G(1323^+)\,. \tag{59}$$

This allows us to eliminate the two-particle Green function, and the integral in Eq. (51) becomes

$$\begin{aligned} & -i\hbar \int v(1^+3) G(1323^+) d3 \\ & = \underbrace{-i\hbar \left(\int v(13) G(33^+) d3 \right)}_{V^{\mathrm{H}}(1)} G(12) + i\hbar \int v(1^+3) \frac{\delta G(12)}{\delta U(3)} d3 \\ & = V^{\mathrm{H}}(1) G(12) + \int \Sigma(13) G(32) d3 \,, \end{aligned} \tag{60}$$

where $V^{\mathrm{H}}(1)$ is the Hartree potential [cf. Eq. (21)] and

$$\begin{aligned} \Sigma(12) &= i\hbar \iint v(1^+3) \frac{\delta G(14)}{\delta U(3)} G^{-1}(42) d3\, d4 \\ &= -i\hbar \iint v(1^+3) G(14) \frac{\delta G^{-1}(42)}{\delta U(3)} d3\, d4 \\ &= i\hbar \iint W(1^+3) G(14) \Gamma(42;3) d3\, d4 \end{aligned} \tag{61}$$

the self-energy. For the second identity we used partial integration and for the third the chain rule for functional derivatives, the definition of the screened interaction (Eq. (58)) and the vertex function

$$\Gamma(12;3) = - \left. \frac{\delta G^{-1}(12)}{\delta U_{\mathrm{eff}}(3)} \right|_{U=0} . \tag{62}$$

With the self-energy (Eq. (61)) the equation of motion for the Green function (Eq. (51)) now becomes

$$\left[i\hbar \frac{\partial}{\partial t_1} - \hat{h}_0(1) \right] G(12) - \int \Sigma(13) G(32) d3 = \delta(12) \,, \tag{63}$$

where we incorporated the Hartree potential into the one-particle operator

$$\hat{h}_0(1) = \hat{h}(1) + V^{\mathrm{H}}(1) \,. \tag{64}$$

The delta function on the right-hand side of Eq. (63) demonstrates that $G(12)$ is indeed a Green function in the mathematical sense. In a noninteracting system the self-energy vanishes, and Eq. (63) becomes

$$\left[i\hbar \frac{\partial}{\partial t_1} - \hat{h}_0(1) \right] G_0(12) = \delta(12) \,. \tag{65}$$

Multiplication of Eq. (63) with G_0 and Eq. (65) with G from the left followed by integration yields the Dyson equation

$$G(12) = G_0(12) + \iint G_0(13) \Sigma(34) G(42) d3\, d4 \,. \tag{66}$$

Finally, Eqs. (65) and (66) allow us to rewrite the vertex function (Eq. (62)) as

$$\Gamma(12;3) = \delta(12)\delta(13) + \frac{\delta \Sigma(12)}{\delta U_{\mathrm{eff}}(3)} \,, \tag{67}$$

and with the identity

$$\begin{aligned}\frac{\delta G(12)}{\delta U_{\text{eff}}(3)} &= \frac{\delta}{\delta U_{\text{eff}}(3)} \iint G(14)G^{-1}(45)G(52)d4\,d5 \\ &= 2\frac{\delta G(12)}{\delta U_{\text{eff}}(3)} + \iint G(14)\frac{\delta G^{-1}(45)}{\delta U_{\text{eff}}(3)}G(52)d4\,d5 \end{aligned} \tag{68}$$

we obtain

$$\Gamma(12;3) = \delta(12)\delta(13) - \iiiint \frac{\delta\Sigma(12)}{\delta G(45)}G(56)\Gamma(67;3)G(74)d4\,d5\,d6\,d7 \tag{69}$$

and analogously

$$P(12) = -i\hbar\frac{\partial G(11^+)}{\partial U_{\text{eff}}(2)} = -i\hbar\iint G(13)\Gamma(34;2)G(41)d3\,d4\,. \tag{70}$$

The Eqs. (58), (66), (61), (69) and (70) constitute Hedin's set of integro-differential equations, whose self-consistent solution, in principle, solves the many-electron problem exactly. Unfortunately, they are not just numerical relations but contain a functional derivative in Eq. (69). Therefore, the Hedin equations cannot be solved self-consistently by computer codes, but they may be iterated analytically in order to derive useful approximations. In practice we can only perform one iteration. We start with the Green function G_0 of the noninteracting system, which corresponds to the single-particle Hamiltonian (Eq. (64)). As the corresponding self-energy vanishes in this case, the set of equations simplifies to

$$\Gamma(12;3) = \delta(12)\delta(13)\,, \tag{71}$$

$$P(12) = -i\hbar G_0(12)G_0(21)\,, \tag{72}$$

$$W(12) = v(12) + \iint v(13)P(34)W(42)d3\,d4\,, \tag{73}$$

$$\Sigma(12) = i\hbar G_0(12)W(1^+2)\,, \tag{74}$$

$$G(12) = G_0(12) + \iint G_0(13)\Sigma(34)G(42)d3\,d4\,. \tag{75}$$

The polarization function here corresponds to the bubble diagram of Feynman's diagrammatic approach to many-body perturbation theory and leads to the random-phase approximation for the screened interaction (cf. Figure 5). The expression for the self-energy in this first iteration coined the name GW approximation.

Appendix B

Quasiparticle equation

Inserting Eq. (12) into the equation of motion for the Green function of a stationary system in the frequency domain

$$\left[\hbar\omega - \hat{h}_0(\mathbf{r})\right] G(\mathbf{r},\mathbf{r}',\omega) - \int \Sigma(\mathbf{r},\mathbf{r}'';\omega)G(\mathbf{r}'',\mathbf{r}';\omega)d^3r'' = \delta\left(\mathbf{r}-\mathbf{r}'\right)\,, \tag{76}$$

which is equivalent to the Dyson equation, yields

$$\sum_i \frac{\psi_i^*(\mathbf{r}')}{\hbar\omega - \epsilon_i \mp i\eta} \left\{ \left[\hbar\omega - \hat{h}_0(\mathbf{r})\right] \psi_i(\mathbf{r}) - \int \Sigma(\mathbf{r}, \mathbf{r}''; \omega)\, \psi_i(\mathbf{r}'')\, d^3r'' \right\} = \delta(\mathbf{r} - \mathbf{r}') \ . \tag{77}$$

Now we multiply with $(\hbar\omega - \epsilon_j)$ and take the limit $\omega \to \epsilon_j/\hbar$ on both sides. If we assume that the system is nondegenerate (i.e., all ϵ_i are different), the left-hand side becomes

$$\lim_{\omega\to\epsilon_j/\hbar} (\hbar\omega - \epsilon_j) \sum_i \frac{\psi_i^*(\mathbf{r}')}{\hbar\omega - \epsilon_i \mp i\eta} \left\{ \left[\hbar\omega - \hat{h}_0(\mathbf{r})\right] \psi_i(\mathbf{r}) - \int \Sigma(\mathbf{r}, \mathbf{r}''; \omega)\, \psi_i(\mathbf{r}'')\, d^3r'' \right\}$$

$$= \psi_j^*(\mathbf{r}') \left\{ \left[\epsilon_j - \hat{h}_0(\mathbf{r})\right] \psi_j(\mathbf{r}) - \int \Sigma(\mathbf{r}, \mathbf{r}''; \epsilon_j/\hbar)\, \psi_j(\mathbf{r}'')\, d^3r'' \right\} , \tag{78}$$

and the right-hand side becomes

$$\lim_{\omega\to\epsilon_j/\hbar} (\hbar\omega - \epsilon_j)\, \delta(\mathbf{r} - \mathbf{r}') = 0 \, . \tag{79}$$

Since $\psi_j^*(\mathbf{r}')$ does not vanish for all $\mathbf{r}'$, the expression in the curly brackets must be zero. This leads directly to the quasiparticle equation

$$\hat{h}_0(\mathbf{r})\, \psi_j(\mathbf{r}) + \int \Sigma(\mathbf{r}, \mathbf{r}''; \epsilon_j/\hbar)\, \psi_j(\mathbf{r}'')\, d^3r'' = \epsilon_j \psi_j(\mathbf{r}) \ . \tag{80}$$

It remains valid in the degenerate case, which is seen as follows. We assume that the solution of Eq. (80) leads to degenerate amplitudes $\psi_j(\mathbf{r})$ and energies ϵ_j. Then we introduce an arbitrary perturbation $\hat{\phi}$, e.g., an additional external potential in $\hat{h}_0(\mathbf{r})$, that breaks the symmetry in such a way that the degeneracy is lifted. For this (nondegenerate) case the above proof applies. The validity of Eq. (80) for the degenerate case is then established by taking the limit $\hat{\phi} \to 0$.

References

1. P. Hohenberg and W. Kohn, *Inhomogeneous Electron Gas*, Phys. Rev. **136**, B864 (1964).
2. A. L. Fetter and J. D. Walecka, *Quantum Theory of Many-Particle Systems* (Dover, New York, 2003).
3. G. D. Mahan, *Many-Particle Physics* (Plenum, New York, 1990).
4. L. Hedin, *New Method for Calculating the One-Particle Green's Function with Application to the Electron-Gas Problem*, Phys. Rev. **139**, A796 (1965).
5. W. Kohn and L. J. Sham, *Self-Consistent Equations Including Exchange and Correlation Effects*, Phys. Rev. **140**, A1133 (1965).
6. L. J. Sham and W. Kohn, *One-Particle Properties of an Inhomogeneous Interacting Electron Gas*, Phys. Rev. **145**, 561 (1966).
7. J. P. Perdew, R. G. Parr, M. Levy, and J. L. Balduz, *Density-Functional Theory for Fractional Particle Number: Derivative Discontinuities of the Energy*, Phys. Rev. Lett. **49**, 1691 (1982).

8. W. G. Aulbur, L. Jönsson, and J. W. Wilkins, *Quasiparticle calculations in solids* in Solid State Physics, edited by H. Ehrenreich and F. Spaepen (Academic, New York, 2000), Vol. 54, p. 1.
9. P. Duffy, D. P. Chong, M. E. Casida, and D. R. Salahub, *Assessment of Kohn-Sham density-functional orbitals as approximate Dyson orbitals for the calculation of electron-momentum-spectroscopy scattering cross sections*, Phys. Rev. A **50**, 4707 (1994).
10. W. von der Linden and P. Horsch, *Precise quasiparticle energies and Hartree-Fock bands of semiconductors and insulators*, Phys. Rev. B **37**, 8351 (1988).
11. G. E. Engel and B. Farid, *Generalized plasmon-pole model and plasmon band structures of crystals*, Phys. Rev. B **47**, 15931 (1993).
12. M. S. Hybertsen and S. G. Louie, *First-Principles Theory of Quasiparticles: Calculation of Band Gaps in Semiconductors and Insulators*, Phys. Rev. Lett. **55**, 1418 (1985).
13. R. W. Godby, M. Schlüter, and L. J. Sham, *Accurate Exchange-Correlation Potential for Silicon and Its Discontinuity on Addition of an Electron*, Phys. Rev. Lett. **56**, 2415 (1986).
14. M. S. Hybertsen and S. G. Louie, *Electron correlation in semiconductors and insulators: Band gaps and quasiparticle energies*, Phys. Rev. B **34**, 5390 (1986).
15. R. W. Godby, M. Schlüter, and L. J. Sham, *Quasiparticle energies in GaAs and AlAs*, Phys. Rev. B **35**, 4170 (1987).
16. J. E. Northrup, M. S. Hybertsen, and S. G. Louie, *Theory of quasiparticle energies in alkali metals*, Phys. Rev. Lett. **59**, 819 (1987).
17. R. Keyling, W.-D. Schöne, and W. Ekardt, *Comparison of the lifetime of excited electrons in noble metals*, Phys. Rev. B **61**, 1670 (2000).
18. G. Onida, L. Reining, and A. Rubio, *Electronic excitations: density-functional versus many-body Green's-function approaches*, Rev. Mod. Phys. **74**, 601 (2002).
19. M. Petersilka, U. J. Gossmann, and E. K. U. Gross, *Excitation Energies from Time-Dependent Density-Functional Theory*, Phys. Rev. Lett. **76**, 1212 (1996).
20. L. Hedin and S. Lundqvist, *Effects of Electron-Electron and Electron-Phonon Interactions on the One-Electron States of Solids* in Solid State Physics, edited by F. Seitz, D. Turnbull and H. Ehrenreich (Academic, New York, 1969), Vol. 23, p. 1.